Synthesis And Characterization Of A New Family Of Hybrid Organic-Inorganic Glasses

Mónica Trejo-Duran, Antonio Martínez-Richa, Ricardo Vera-Graziano, Victor M. Castaño

Addresses for Correspondence: M. Trejo-Duran, V. Castaño, Centro de Física Aplicada y Tecnología Avanzada, UNAM, Apdo. Postal 1010, Querétaro, Qro. 76001, México; A. Martínez-Richa, Facultad de Química, Universidad de Guanajuato, Noria Alta s/n, Guanajuato, Gto, 36050 México; R. Vera-Graziano, Instituto de Investigaciones en Materiales, UNAM, Apdo. Postal 70-360, Coyoacán, 04510, México, D. F.; V. Castaño, meneses@servidor.unam.mx

Received: 23 August 2004 Revised: 04 August 2005 Accepted: 23 September 2004

Keywords: *Hybrids Fluorescence Sol-gel process Siloxane NMR*

Introduction

Relation To Previous Work

The design of new hybrid materials constitutes an attractive research area for the development of new materials with enhanced properties. In particular, organic-inorganic hybrids and Ormosils are promising materials to be used in optics and electro-optics [1–18]. There is also current interest in the development of nanometric amorphous materials with unique optical properties, in particular the study of the sizes of hybrid materials is an active research field.

Many organic-inorganic hybrid materials are prepared by introducing a polymeric component into a silica environment using the sol-gel process [19–24]. This technology is of particular interest due to the large number of chemical and structural modifications available and to the possibility of developing novel materials, which combine the characteristics of both components.

The Sol-Gel technique has been promising since the beginning in the development of new materials [25]. The sol-gel process offers many advantages such as matrix uniformity, better particle size control and low processing temperatures. Because the sol-gel process initiates in liquid state, hybrid materials in both bulk and film forms can be successfully prepared. However, some problems could arise during the formation of the final product. For example, glass composites prepared by this method yield porous and brittle materials susceptible of cracking during the drying step. To avoid this problem, the proper conditions for glasses should be carefully determined by experimentation.

Nowadays, the use of polysiloxanes in the production of electro-optics devices is a common practice in industry [19, 22, 23]. Most polysiloxanes have two important characteristics: a low glass transition temperature and elastomeric properties. Recently, polysiloxanes with various mesogenic side-chain units have been synthesized and used as stationary phases in gas chromatography; some of them having a cyano functionality in the organic component. Usually, mesogens with cyano groups are strongly polar nematic

compounds with positive dielectric anisotropy, and show a twisted nematic effect. Some attempts have also been made to produce poly(cyano siloxanes) intended for display devices [26].

The aim of the present work is to synthesize a new family of fluorescent hybrid materials, with potential applications in optics, that combine the characteristics and properties of organic-inorganic hybrid materials with those of polysiloxanes. Here we describe the synthesis and characterization of hybrids prepared by the sol-gel technique where nanometric silica particles form the inorganic phase and an aromatic siloxane with a cyano subtituent the organic component.

Experimental

Materials. 4-cyanophenol, 5-Bromo-1-pentene, hexachloroplatinic acid and dichloromethylsylane were purchased (Aldrich) and used as received as well as were others chemicals and solvents.

Techniques. A 200 MHz Varian Gemini 2000 spectrometer was used to obtain the ^{1}H NMR and ^{13}C NMR at room temperature. A 300 MHz Varian Unity Plus spectrometer was used to obtain ^{29}Si NMR in solution (using INEPT sequence) and in the solid state, TMS was used as the internal standard. An Olympus BX40 (Dilor) was used to obtain Micro-Raman spectra with 50x objective and He-Ne laser at 632.8 nm. Raman spectra were recorded on a Nicolet Raman 910 spectrometer with 100 scans. An Atomic Force Microscope, Digital Instruments Nanoscope 111a, with a Dimension 3100 controller, was used to record the AFM micrographs. FTIR spectra were recorded in a Perkin-Elmer 1600 series using film over KBr and KBr pellets with 16 scans. UV spectra were recorded on a Perkin-Elmer Lambda 40 UV/Vis spectrometer. A Transmission Electron Microscope, JEOL 1010, 80 KV was used to obtain TEM micrographs.

Synthesis of [4-(((5-dichoromethylsilyl)pentyl)oxy)-cyanobencene] (DCN). DCN precursor was prepared from [4-cyanophenol] and [5-bromo-1-pentene] in acetone and potassium carbonate at 50 °C for 24 h. After purification, the [4-[pentenyl]oxy]-cyanobencene] was hydrosylilated with dichloromethylsylane in toluene using chloroplatinic acid as catalyst. The mixture was refluxed for 16 h at 58 °C until the reaction was completed, then the product was distillated to obtain DCN isolated (see Scheme 1): IR (neat) 2937 (aromatic, -CH), 2864 (-CH_2-acyclic), 2224 (CN group), 1606 and 1508 (p-substituted aromatic ring), 1301 (R-O-Ar), 1260 (C-O-C) , 1171 (C-O), 834 (ar –H deformation), 807 (Si-CH_3), 732 and 696 (Si-CH_2), 546 (Ar-CN), 527 and 465 (Si-Cl_2) cm $^{-1}$[26].

Raman (neat) 3070 (aromatic, -CH, stretch), 2902 (CH_3), 2966 (CH_2 sym and asym), 2217 (CN stretch), 1597 (p-substituted aromatic), 1294 (C-O-C stretch), 1249 (Si-CH_3), 1197 (Si-CH_2 wag, twist), 1165 (C-O-C sym stretch), 855 and 803 (Si-Cl), 829 (aromatic, CH out plane), 739 (Si-CH_2), 538 (Cl-Si-CH_3), 474 (C-O-C) cm^{-1}.
^{1}H NMR ($CDCl_3$): δ 7.59-6.88 (d de t, AA'BB',4 H, aromatic), 4.00 (t, 2 H, -OCH_2), 1.89-1.15 (3m, $(CH_2)_4$), 0.79 (3H, -CH_3). ^{13}C NMR ($CDCl_3$): δ 119.23 (CN), 103.69 (NC-C, aromatic), 133.90 (C_b, aromatic), 115.12 (C_c, aromatic), 162.30 (C-O, aromatic), 67.45 (O-CH_2), 29 – 21.5, (methylenes), 5.8 (Si-CH_3). ^{29}Si NMR ($CDCl_3$) 32.6 (CH_3-*Si*-).
UV-vis in THF 246 nm (aromatic, $\pi \rightarrow \pi^*$), 284, 363 and 314 nm ($\eta \rightarrow \pi^*$ transitions).

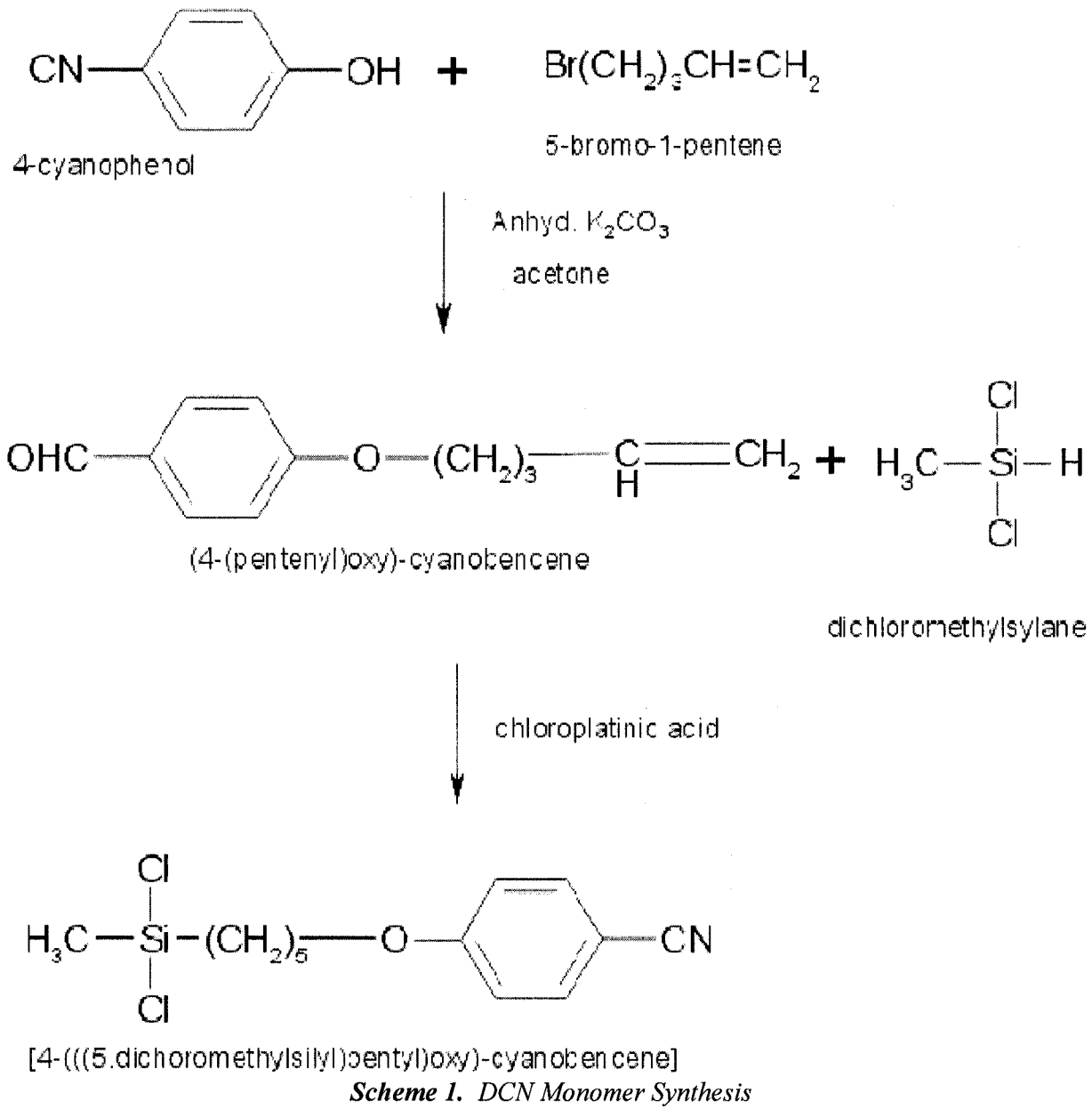

Scheme 1. *DCN Monomer Synthesis*

Synthesis of organic-inorganic glass hybrids. The TEOS was dissolved in THF and treated with nitric acid. To this solution, water was slowly added for 10 min under continuous stirring. The DCN monomer (dissolved in toluene at 20%) was slowly added to the mixture using a syringe provided with a hypodermic needle. The reaction mixture was heated under nitrogen atmosphere for 18 h (See Scheme 2). Reaction conditions to prepare hybrids are shown in Table 1.

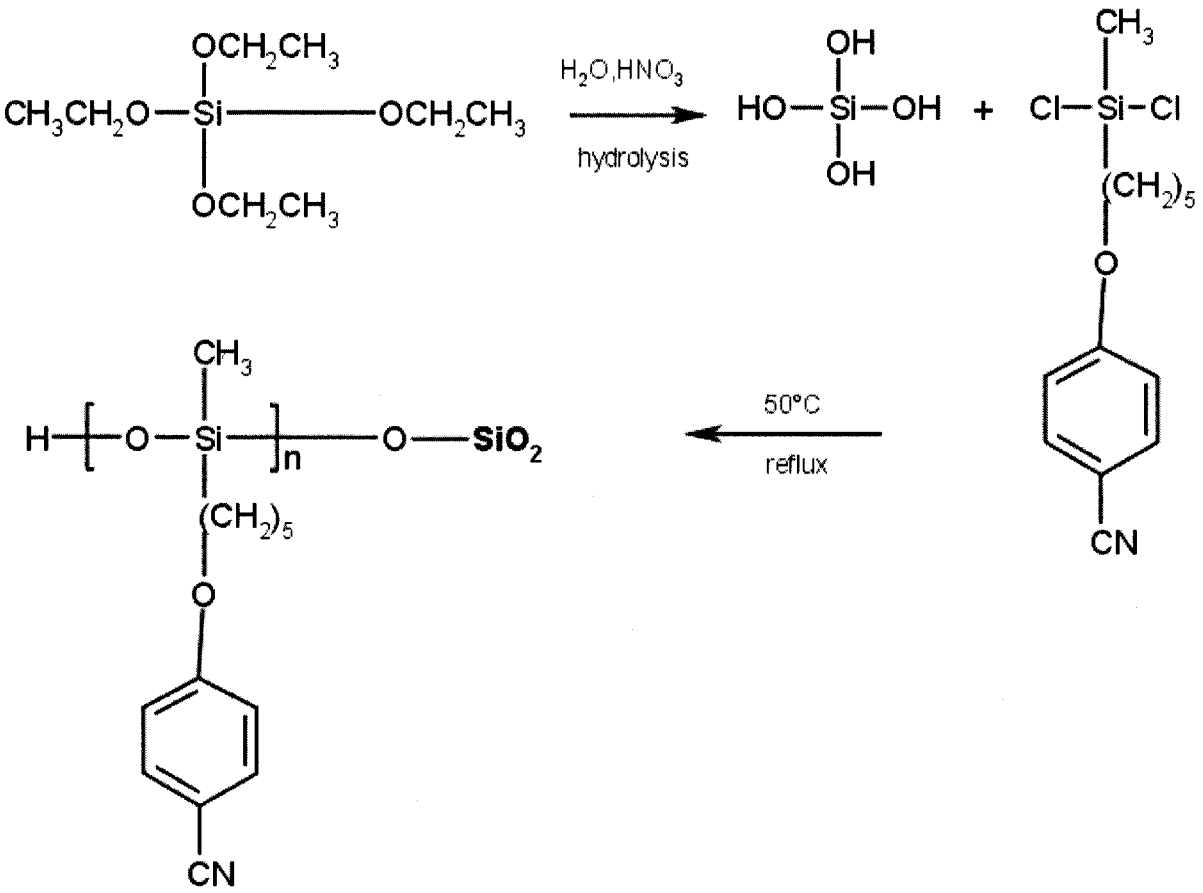

Scheme 2. *Hybrid Synthesis*

Gel time and phase separation depended upon the concentration of DCN [27, 28]. The final materials were recovered as monoliths that took the form of the mold, and transparent to opaque yellow solid monoliths of homogeneous appearance were obtained depending upon the reaction temperature. The hydrolysis reaction occurred very quickly under strong acidic conditions and the formed silica was extensively condensed.

Results And Discussion

Figure 1 shows the FT-IR spectra of the hybrids in solid-state. Note that the intensity of the peak at 2224 cm^{-1} depends upon the concentration of the DCN monomer. In the spectra, the peak of the silica spectra were normalized with respect to Si = 0 peak at 1074 cm^{-1}. Figure 2 shows the FT-IR spectra of hybrid A before gelation and in solid-state. Peaks are observed at 3418 cm^{-1} (corresponding to Si-OH), 2932 cm^{-1} (CH_3, CH_2), 2226 cm^{-1} (CN group), 1606 and 1508 cm^{-1} (p-substituted aromatic ring), 1301 (R-O-Ar), 1262 cm^{-1} (C-O-C), 1171 (C-O), 1074 cm^{-1} (Si-O-Si), 834 (aromatic –H deformation), and 548 (Ar-CN). Notice that all signals are broader in the solid-state spectrum, as a consequence of the polymerization process. The silanol peak shows a higher relative area and is broader in the polymer spectrum.

The samples were also analyzed by solution and solid- state NMR. Solution ^{1}H NMR, ^{13}C NMR and ^{29}Si NMR spectra of the hybrids before gelation are shown in Figs. 3, 4 and 5.
In the Proton and Carbon 13 spectra, signals for oligomeric species are observed (Fig. 5). The ^{29}Si NMR spectrum of hybrids have peaks at -20.11, -20.25 and -22.45 ppm that correspond to the D units, and the peaks at -65 pm correspond to the T units. No signal for silica was observed in these spectra.

The CP-MAS and MAS ^{29}Si NMR spectra of the hybrids A and B are shown in Fig. 6. The signal around -100 ppm, corresponding to fully condensed units, Q^4, is the largest peak in the spectrum. The signal at -93 ppm corresponds to Q^3 units (units with one uncondensed silanol). No signals corresponding to Q^2 units (units with two uncondensed silanols) are present.

The Q^3 units were better resolved in the CP-MAS spectrum of both hybrids (Fig. 6b). This is due to the polarization transfer from the proton to the silicon nuclei which possess higher sensitivity in the Q^3 units because hydrogen is closer to silicon (in the Si-OH group) than the Q^4 units, where H nuclei are located farther. The areas under the peaks indicate that the ratio Q^4/ Q^3 is above 1 (See Figure 6-(1) b). This means that the major part of the silica was condensed as Q^4 units. Figure 6-(2)-b shows the solid-state spectra for hybrid A. Areas under the peaks for ratio Q^4/ Q^3 are less than 1. In this case, the majority of silicas were condensed as Q^3 units.

The formation of a random copolymer formed by arylalkylsiloxane groups (DCN) and silica is evident in the observation of a peak at around -10 ppm in the solid-state ^{29}Si NMR spectra of the hybrids (marked as D, Fig. 6) [22,29]. The signal at –55 ppm (marked as T^2) was assigned to silanol groups, Si-OH. The peak corresponding to T^2 units in the MAS spectrum was lower than that observed in CP-MAS, because again, silanol groups, Si-OH, have the H nuclei closer to the Si. The formation of Si-OH groups is favored in concentrated acidic conditions. Notice the difference of signals T^2 and Q's between hybrids in Fig. 6. Hybrid B spectra shows a higher signal T^2 than that observed in hybrid A spectra. These differences are mainly due to reaction temperature. In these spectra the Q's signals are narrower than those observed for silica obtained by the sol-gel process.

Raman and micro-Raman spectroscopy provided clear evidence of fluorescence in the prepared hybrids. The Raman and micro-Raman spectra are shown in Fig. 7 and 8 respectively. In Fig. 7a and 7b, peaks observed at 2907 (CH_2 str. aromatic ring), 2225 (CN group), 1606 cm^{-1} (aromatic), and 836 (CH_2 bend wag) corresponded to the polymer. The peak at 480 cm^{-1} was due to silica bonds. Figure 8a shows the Micro-Raman spectra obtained at different domains in the hybrids B surface. It was evident that the extent of fluorescence depended upon the observed domain. A similar behavior was observed in the others hybrids obtained. The micro-Raman spectra in Fig. 8b corresponded to different type of hybrids; the same peak pattern was observed, but the extent of fluorescence did not vary linearly and depended of the concentration of the siloxane component.

The morphologies of the hybrids B and A were studied by transmission electron microscopy (TEM). A sample from hybrid C, a specimen 10 nm thick obtained from the center of the sample, was obtained with a microtome. The TEM was recorded directly from powder due to the characteristics of its physical state.
The micrograph of Fig. 9a shows a nano-porous structure made of aggregated particles in a continuous matrix. The particles are aggregated in a disorderly fashion and porosity appears at the particles interstices.

This morphology is different from the features observed in most silica gel samples where only grain features are present. The average range diameter of the particles is 25–50 nm, which is lower than the range of silica particle sizes prepared from TEOS.
The micrograph of Fig. 9b shows a structure of a continuous matrix with fringes; dark fringes correspond to crystalline arrays, where as light fringes correspond to the "copolymer" in the amorphous state. The average range diameter of the particles is similar to that shown in Fig. 9a, but its arrangement is different due to conditions reactions. The small dimensions of these domains can be attributed to the severe hydrolysis conditions induced by the concentrated acidic medium.

The surface of hybrids was studied by atomic force microscopy (AFM) (Fig. 10). The micrograph of hybrid B, (Fig. 10a) shows a rough surface with cone shaped nano-holes. A surface of 323 nm was analyzed, with a horizontal distance (L)= 316 nm and vertical distance = 6. The micrograph of hybrid A, (Fig. 10b) shows a similar surface texture as hybrid B, but nano-holes have smaller dimensions. A surface of 1 nm was analyzed, horizontal distance (L)= 0.3 nm and vertical distance = 0.9 nm. In both hybrids a fringe pattern is present. This pattern is an optical effect possibly due to interference with the fluorescence in the surface.

Conclusions

The synthesis and characterization of a new family of nano-porous hybrids obtained from tetraethoxysilane and 4-[[5-dichoromethylsilyl]pentyl]oxy]-cyanobencene monomer, is reported for the first time. The DCN units are chemically bonded to the silica particles in a copolymer random arrangement.

The NMR spectra evidence the formation of a hybrid in which the 4-[[5dichloro methylsilyl]pentyl]oxy]-cyanobenzene units form a copolymer with silica. Raman spectra also indicate that the hybrids show fluorescence. Fluorescence is present even at wavelengths where absorption bands do not exist. Intensities in the micro-Raman spectra on the surface differ by about 30%. Fluorescence intensity and dimensions of holes in the surface depend on the amount of DCN and temperature used. The presence of copolymer in the surface produces an optical effect (fringes) in the AFM micrographs. Morphology corresponds to that of a nano-porous material made of nanometric particles of the copolymer formed between silica and DCN (25–50 nm).

Acknowledgments. We are indebted with Dr. Sergio Calixto (CIO Leon, Gto) for the AFM micrographs, Dr. Sergio Jimenez (Cinvestav, Qro) for the Micro-Raman spectroscopy spectra, Dra. Genoveva Hernández (CFATA, UNAM) for the Raman spectroscopy spectrum, and Dra. Alicia del Real (CFATA, UNAM) for the TEM micrographs. M.T.D would like to thank CONACyT (Consejo de Ciencia y Tecnologia) for the scholarship.

REFERENCES

1. Dalton LR, Harper AW, Zhu J, Steier WH, Salovey R, Wu J, Efron U (1995) SPIE 2528:106
2. Sanchez C, Lebeau B (1996) Pure Appl Opt 5(5):689
3. Levy D (1996) Pure Appl Opt 5:621
4. Levy D (1997) SPIE Sol-gel Optics IV 3136:77
5. Andrews Mark P (1997) SPIE Integrated Optics Devices; Potential for Commercialization 2997:48
6. Boilot J-P, Biteau J, Chaput F, Giacoin T, Brun A, Darracq B, Georges P, Levy Y (1998) Pure Appl Opt 7(2):169
7. Canva M, Darracq B, Chaput F, Lahlil K, Bentivegna F, Brunel M, Falloss M, Georges P, Brun A, Boilot J-P, Levy Y (1998) SPIE Organic-Inorganic Hybrid Materials for Photonics 3469:164
8. Harper AW, Sun S, Dalton LR, Garner SM, Chen A, Kalluri S, Steier WH, Robinson BH (1998) J Opt Soc Am B 15(1):329
9. Horowitz F, Alcantara PA, Pereira MB, Campo LF, Stefan V (1999) SPIE Organic Photorefractives, Photoreceptors, Waveguides, and Fibers 3799:49

10. *Tsai I-C, Lin Y-H, Hung M-C, Hong J-Y, Jang G-W (2001) Proceeedings of SPIE Optical Fiber and Planar Waveguide Tech 4579:92*
11. *Laczka M, Cholewa-Kowalska K, Kogut M (2001) J of Non-cristallyne Solids 28:710*
12. *Mackenzie JD (1990) Proc SPIE, Sol-gel Optics 1328*
13. *Cheng C-H, Xu Y, Mackenzie J (1992) SPIE, Sol-Gel Optics II 1758:485*
14. *Li C-Y, Tseng JY, Morita K, Lechner C, Hu Y, Mackenzie JD (1992) SPIE, Sol-Gel Optics II 1758:410-419*
15. *Li Chia-Yen, Wilson M, Haegel N, Mackenzie J, Knobbe ET, Porter C and Reeves R (1992) SPIE 1692:218*
16. *Harried JH, Dunn B, Zink JI (1997) SPIE 3136:25*
17. *Gurney A, Vargas-Baca I, Brown AP (1998) SPIE Organic-Inorganic Hybrid Materials for Photonics 3469*
18. *Atkins GR, Krolikowska R Maryla, Samoc A (1999) SPIE 3803:142*
19. *Tseng JY, Li C-Y, Takada T, Lechner C, Mackenzie JD (1992) SPIE 1758:612*
20. *Burzynski R, Casstevens MK, Zhang Y (1993) SPIE, Organic and Bio Optoelectronics 1853:158*
21. *Mimura S, Naito H, Kanemitsu Y, Matsukawa K, Inoue H (2000) J of Luminiscence 87-89:715*
22. *Jiang S, Ji X, An L, Jiang B (2001) Polymer 42:3901*
23. *Chevalier Y, Grillet A-C, Rahmi I, Liere C, Masure M, Hemery P, Babonneau F (2002) Materials Sci & Engrg C 21:143*
24. *Han Y, Lin J, Zhang H (2002) Mater Let 54:389*
25. *Roy R (1987) Sci 238:1664*
26. *Subramaniam G, Gilpin RK (1990) Macromolecules 23(3):693*
27. *Lobnik A, Wolfbeis O (1997) SPIE 3136:264*
28. *Brus J, Kotlik P (1996) Chem Mater 8:2739*
29. *Brus J, Dybal J (1999) Polymer 40: 6933*

Hybrids type	TEOS:THF:DCN	Reaction Temperature	Number of phases observed	Gelation Time	Physical Appearance
A	1:1:1.0	50°C	2	24 hrs.	Semi-Transparent
B	1:1:0.7	23°C	2	24-48 hrs.	Opaque
C	1:1:0.4	50°C	1	3-4 weeks.	Transparent

Table 1. *Reactions Conditions to prepare a family of hybrids.*

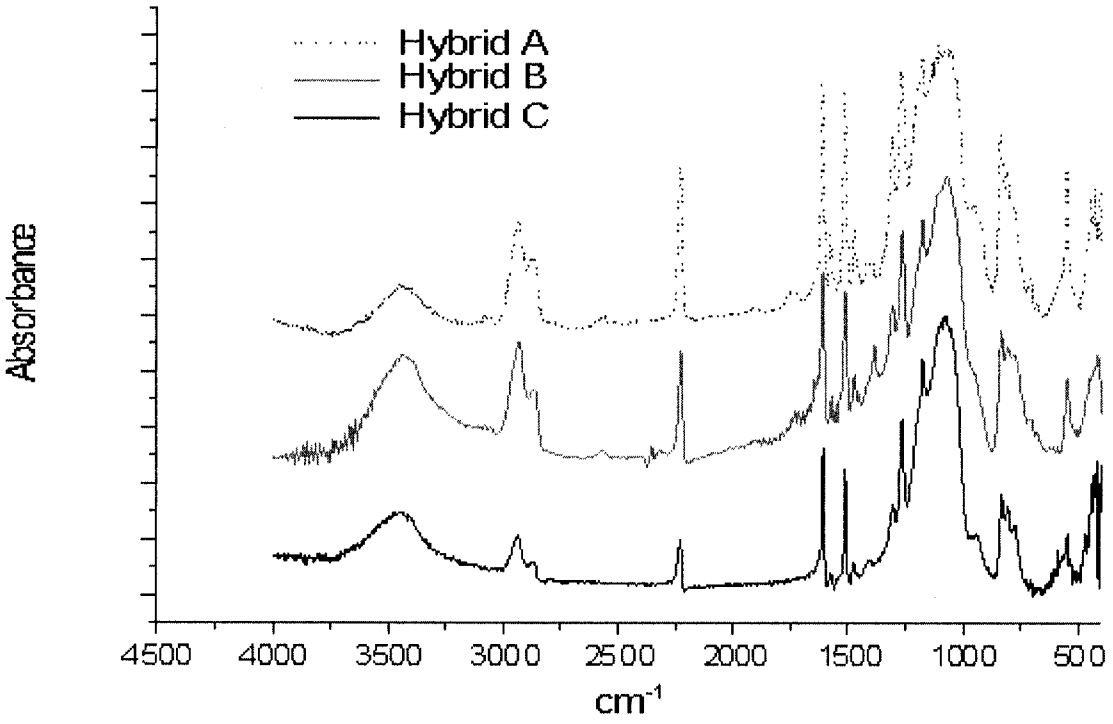

Fig. 1. *FT-IR spectra of hybrids family in solid-state*

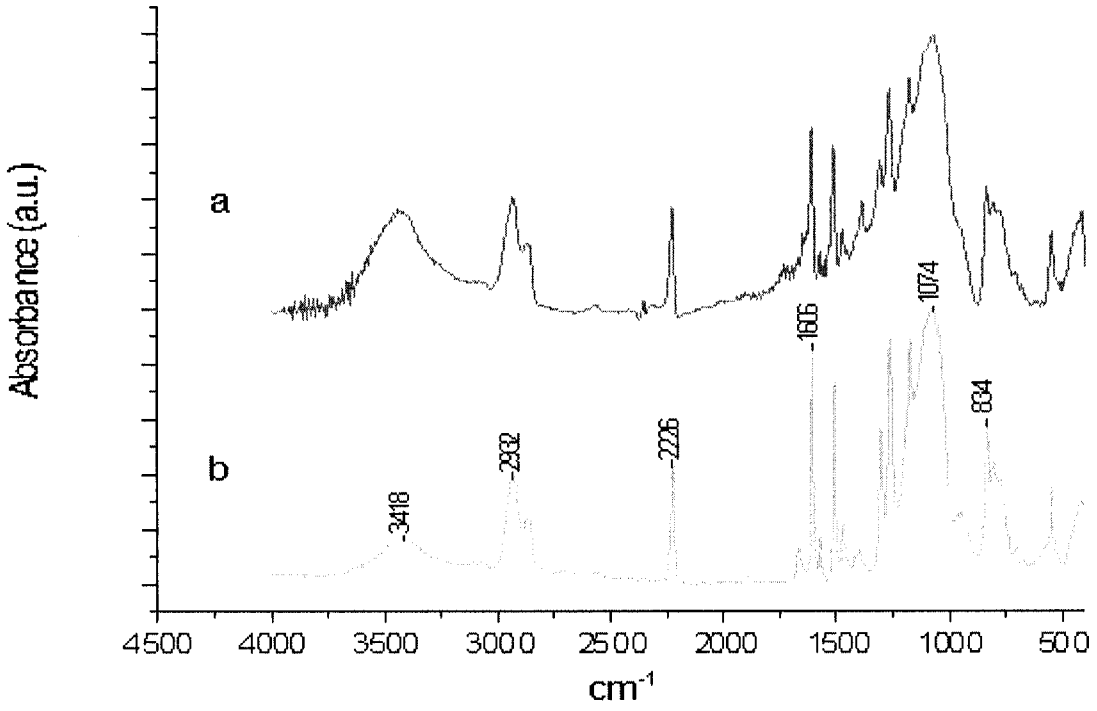

Fig. 2. *FT-IR spectra of hybrid A (a) before gelation and (b) after gelation.*

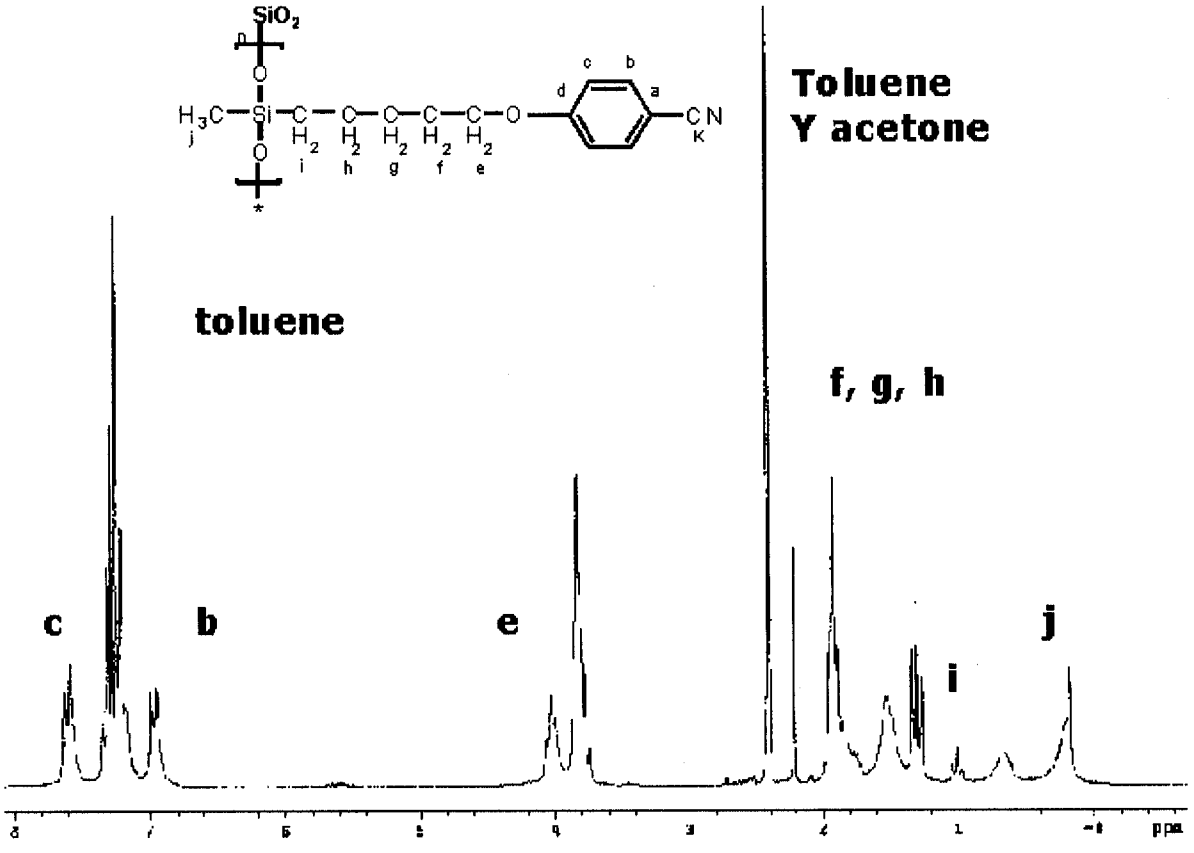

Fig. 3. *^1H NMR spectrum in $CDCl_3$ of hybrids before gelation*

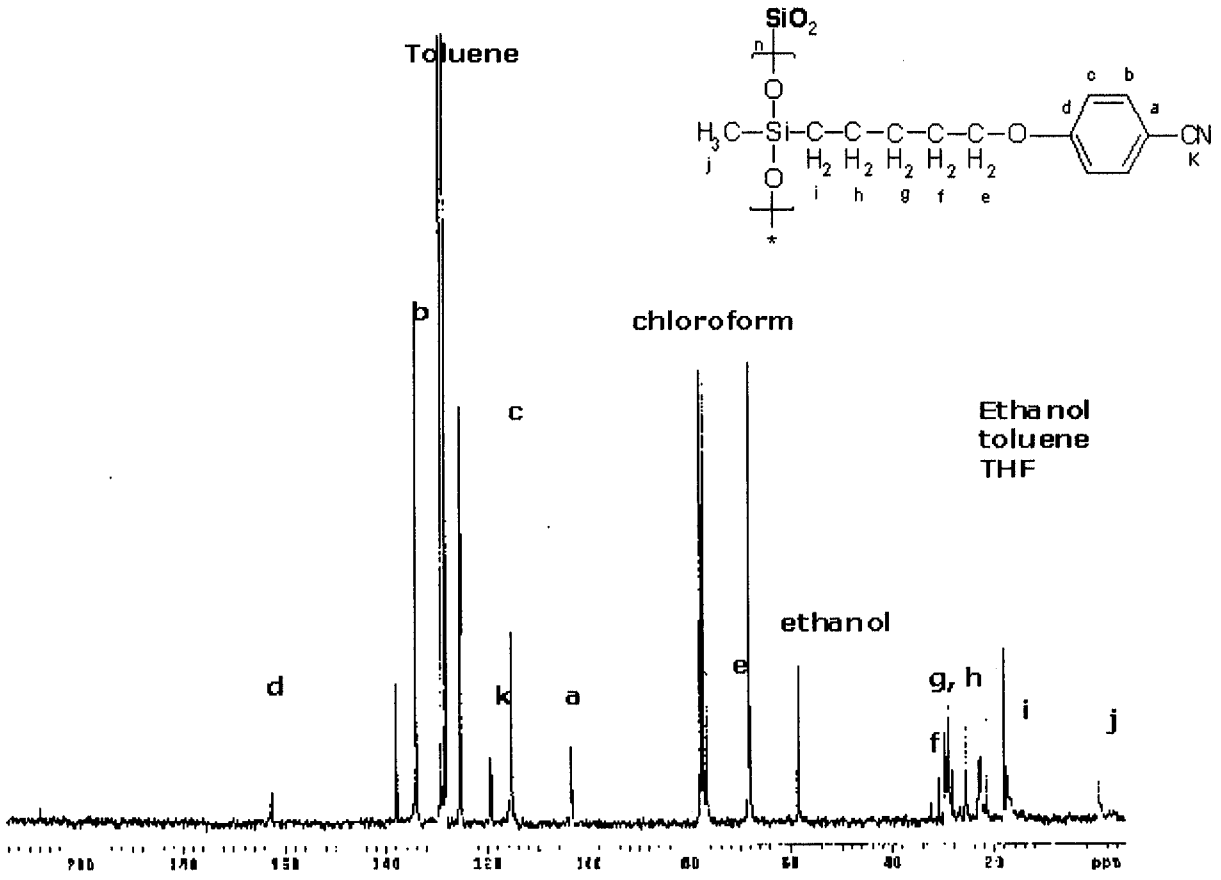

Fig. 4. ^{13}C *NMR spectrum in* $CDCl_3$ *of hybrids before gelation*

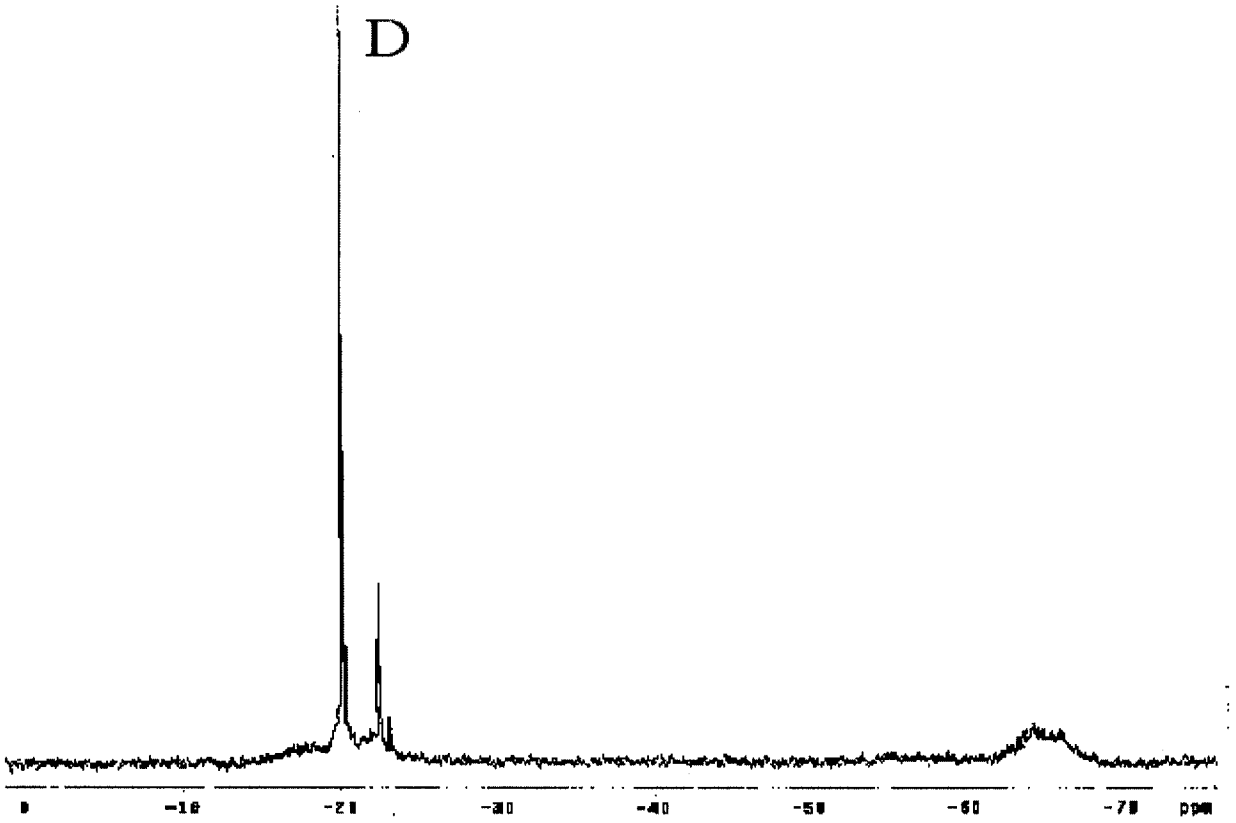

Fig. 5. ^{29}Si *NMR spectrum in* $CDCl_3$ *of hybrids before gelation*

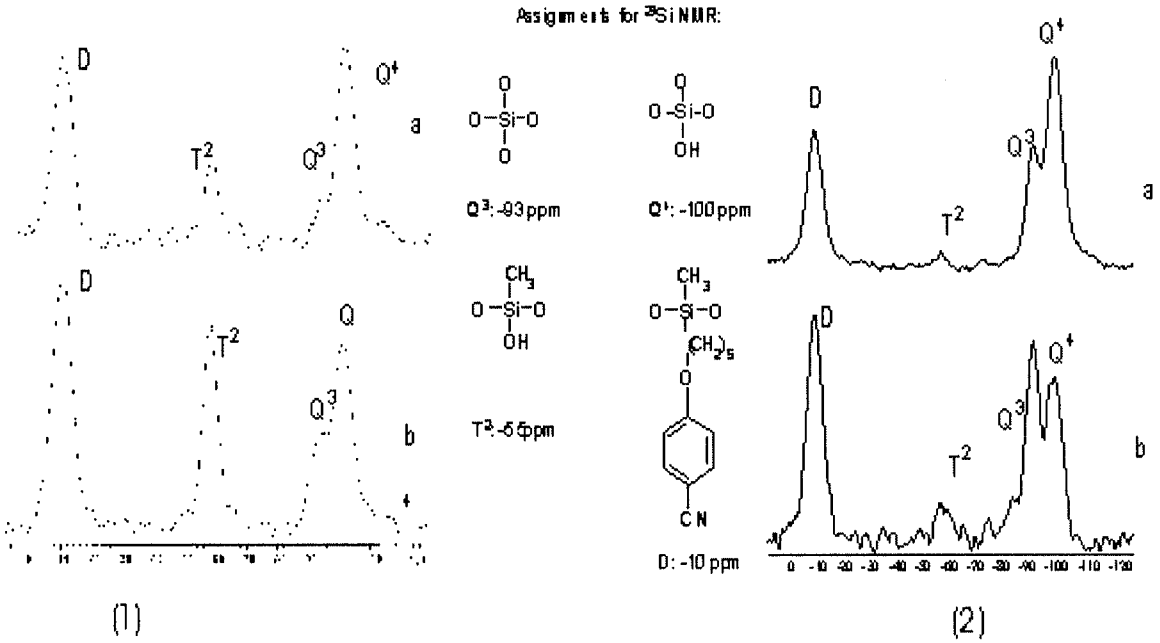

Fig. 6. *^{29}Si solid state NMR spectra of hybrids (1) hybrid B, (2) hybrid A; (a) MAS spectrum (b) CP-MAS spectrum*

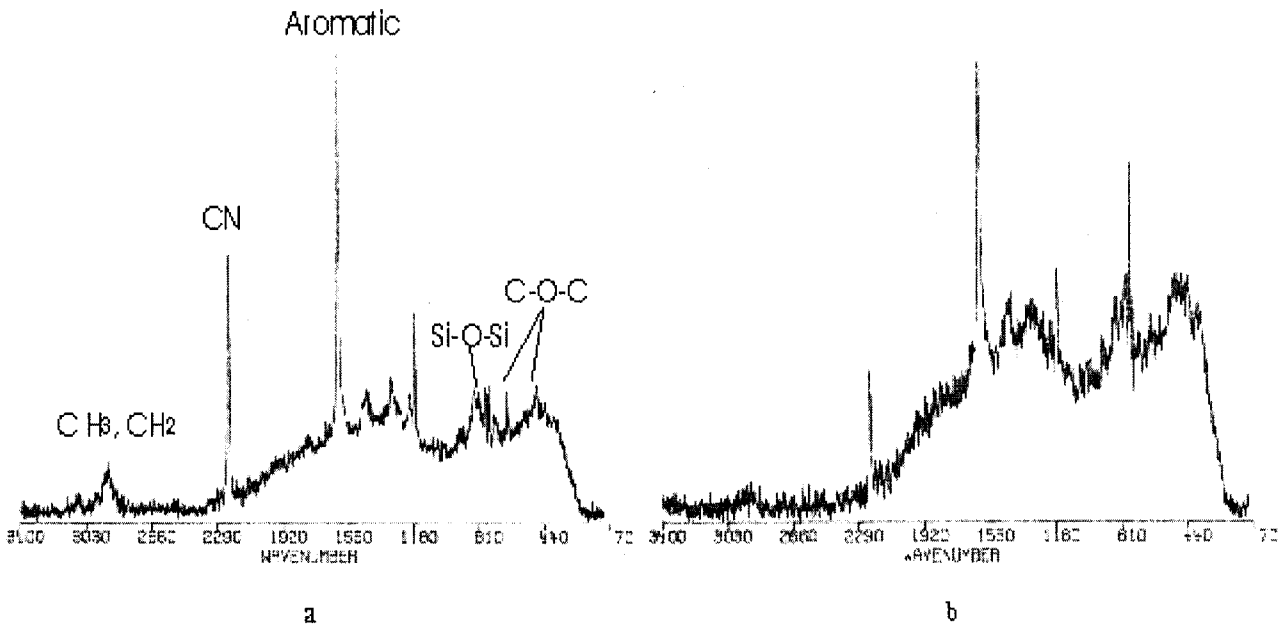

Fig. 7. Raman spectra a) Hybrid B , b) Hybrid A.

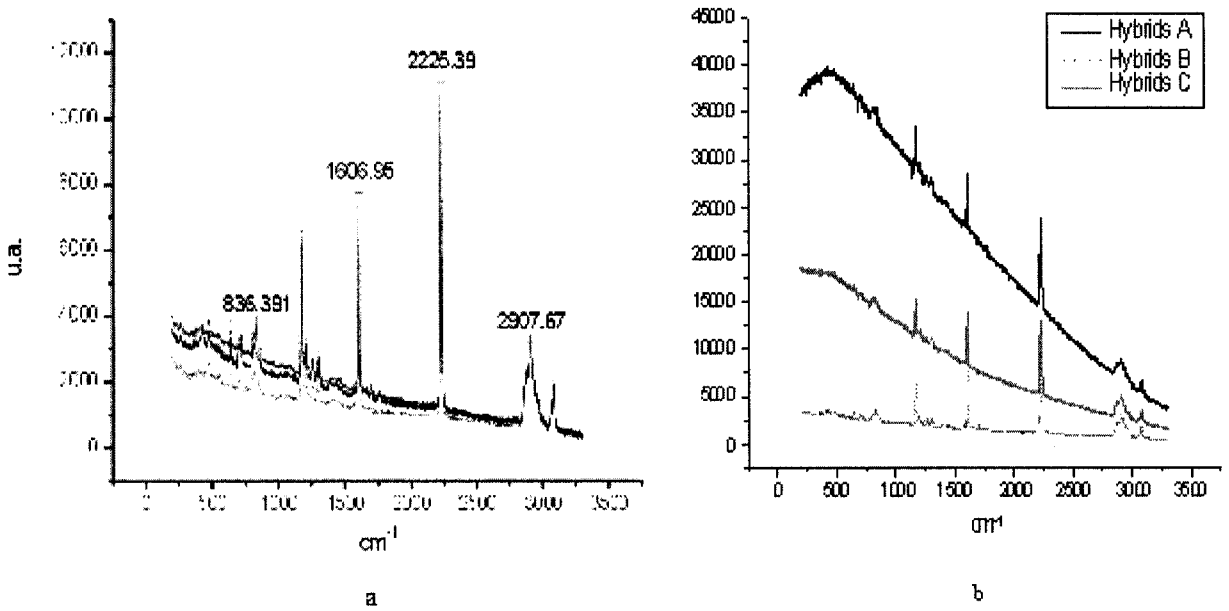

Fig. 8. *a) Micro-Raman spectra of hybrids B obtained in a different surface location of the hybrids, b) Micro-Raman spectra obtained in different types of hybrids*

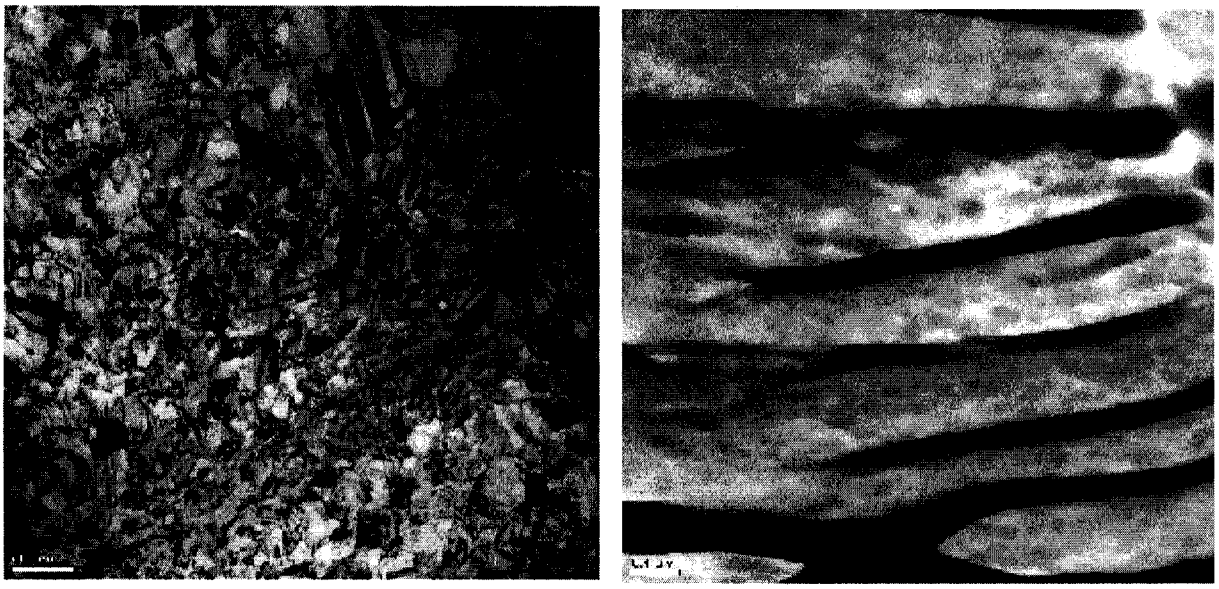

Fig. 9. *Transmission electron micrographs at 20,000x magnification of the sliced hybrids sample. A) Hybrid B, b) Hybrid A*

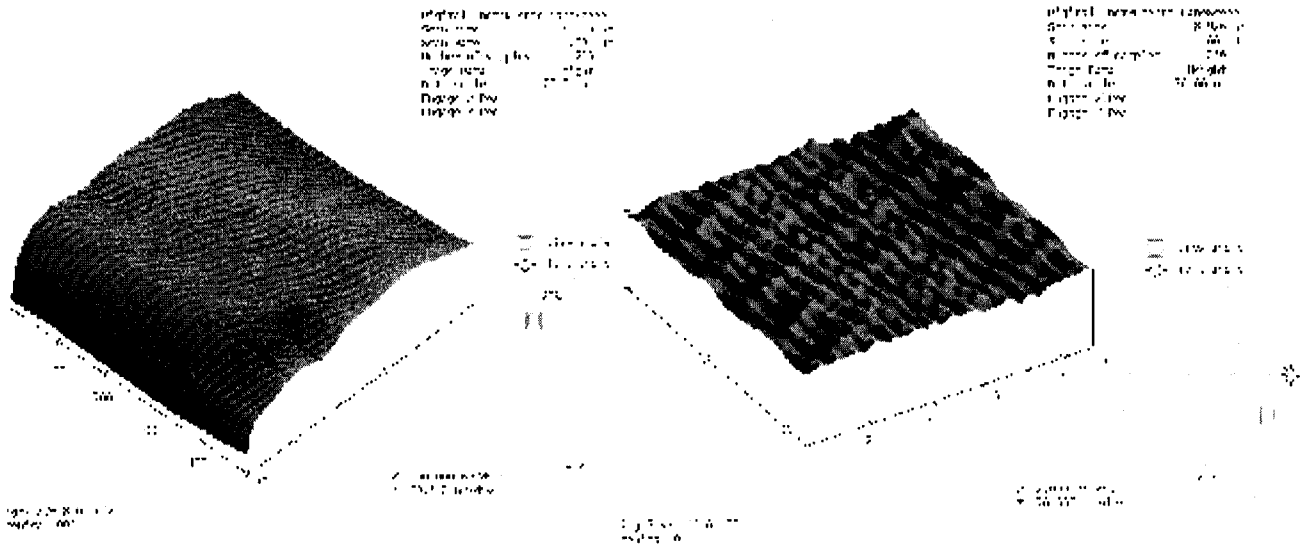

a b

Fig. 10. *Atomic Force Microscope micrographs: (a) Hybrid B, 500x500 nm, (b) Hybrid A, 510 x10 nm*